Int. J. Nav. Archit. Ocean Eng. (2015) 7:324~345
http://dx.doi.org/10.1515/ijnaoe-2015-0023
pISSN: 2092-6782, eISSN: 2092-6790

A new finite element formulation for vibration analysis of thick plates

Ivo Senjanović[1], Nikola Vladimir[1] and Dae Seung Cho[2]

[1]*University of Zagreb, Faculty of Mechanical Engineering and Naval Architecture, Zagreb, Croatia*
[2]*Pusan National University, Dept. of Naval Architecture and Ocean Engineering, Busan, Korea*

ABSTRACT: *A new procedure for determining properties of thick plate finite elements, based on the modified Mindlin theory for moderately thick plate, is presented. Bending deflection is used as a potential function for the definition of total (bending and shear) deflection and angles of cross-section rotations. As a result of the introduced interdependence among displacements, the shear locking problem, present and solved in known finite element formulations, is avoided. Natural vibration analysis of rectangular plate, utilizing the proposed four-node quadrilateral finite element, shows higher accuracy than the sophisticated finite elements incorporated in some commercial software. In addition, the relation between thick and thin finite element properties is established, and compared with those in relevant literature.*

***KEY WORDS*:** Mindlin plate theory; Finite element formulation; Thick-thin plate relation; Vibration analysis; Shear locking.

INTRODUCTION

In plate theory, two mathematical models are distinguished, the well-known Kirchhoff thin plate and the Mindlin thick plate theory. In the former, shear influence on deflection is small and is therefore ignored. This theory is very well developed and the achievements are presented in Szilard's fundamental book (Szilard, 2004). The dynamic behaviour of thick plate is quite a complex problem, due to shear influence and rotary inertia, and is still an interesting subject of investigation. The first works are those of Reissner and Mindlin (Reissner, 1945; Mindlin, 1951), in which it is assumed that the plate cross-section remains a plane but not normal to the plate middle surface. As a result, the Mindlin theory deals with a system of three differential equations of motion with plate deflection and two angles of rotation of cross-section as unknown variables. This system is the starting point for all later developed variants. In the meantime, a large number of articles have been published and a comprehensive survey of literature up to 1994 can be found in (Liew et al., 1995).

Generally, there are two main approaches for solving the problem of thick plate natural vibrations, i.e. analytical methods for the solution of differential equations of motion, and numerical procedures based on the Rayleigh-Ritz energy method as well as the Finite Element Method (FEM). Different analytical methods are known depending on which functions are kept as fundamental ones in the reduction of the system of differential equations of motion. Some methods operate with three, two or even one function, for instance Wang (1994), Shimpi and Patel (2006) Endo and Kimura (2007) and Xing and Liu (2009), respectively. The application of analytical methods is relatively simple for simply supported plates and plates with simply supported two opposite edges. A sophisticated closed-form solution is derived in Xing and Liu (2009) for plate vibration analysis with any

Corresponding author: *Nikola Vladimir*, e-mail: *nikola.vladimir@fsb.hr*

combination of simply supported and clamped edges.

The Rayleigh-Ritz method is widely used for arbitrary boundary conditions as well as for elastically supported edges. Accuracy depends on the chosen set of orthogonal functions for the assumed natural modes. For that purpose two dimensional polynomials can be used Liew et al. (1993), or functions of static Timoshenko beam deflection Dawe and Roufaeil (1980), Cheung and Zhou (2000). Efficient solution is also achieved applying the assumed mode method with static Timoshenko beam functions to thick bare plate Kim et al. (2012) as well as for some more complex problems (Cho et al., 2013; 2014).

The finite element method is a very powerful tool for the analysis of any problem (linear, nonlinear, static and dynamic) of engineering structures with a complicated configuration. Several finite elements for Mindlin plate have been developed and incorporated in commercial FEM software. They deal with three displacement fields, i.e. deflection and two rotations. Due to the impossibility to prescribe correct interdependence among deflection and rotations, the same order polynomials for the interpolation of all displacements are used. Consequently, so-called shear locking phenomenon arises since in transition from thick to thin plate, it is not possible to capture pure bending modes and zero shear strain constraints. There are a few procedures for solving shear locking problem in the FEM analysis, which are referred to in Falsone and Settineri (2012): reduced integration for shear terms (Zienkiewicz et al., 1971; Hughes et al., 1977), which is commonly used in commercial software; mixed formulation of hybrid finite elements (Lee and Wong, 1982; Auricchio and Taylor, 1995; Lovadina, 1998); Assumed Natural Strain (Hughes and Tezduyar, 1981; Bathe, 1996; Zienkiewicz and Taylor, 2000); and Discrete Shear Gap (DSG) (Bletzinger et al., 2000), and its combination with the mesh-free procedure (Liu et al., 2009; Nguyen-Xuan et al., 2010). Recently, a new shear locking free finite element formulation for static analysis of thick plate has been proposed in (Falsone and Settineri, 2012) based on an extension of the well-known Kirchhoff thin plate theory. The so-called fictitious deflection is used as a basic function, by which the other kinematic and static quantities are determined. It is also necessary to mention the worthwhile formulation of the mixed FEM and the Differential Quadrature Method (DQM) for longitudinal and transverse plate direction, respectively (Eftekhari and Jafari, 2013).

Motivated by the state of the art described above, in the present paper a new finite element formulation is proposed for thick plate vibration analysis. It is based on a new moderately thick plate theory presented in (Senjanović et al., 2013a; 2013b), where a system of governing differential equations of motion is reduced to one equation with bending deflection as an unknown function. It is actually a potential function by which total deflection and angles of rotations are determined, as well as bending and shear strains and sectional and inertia forces. This plate theory actually represents an extension of the modified Timoshenko beam theory (Senjanović and Fan, 1989; Senjanović and Grubišić, 1991; Senjanović et al., 2009; Senjanović and Vladimir, 2013). Due to strong interdependence among deflection and rotations, the shear locking phenomenon does not occur. Finite element stiffness and mass matrices are determined by employing an ordinary variational formulation (Zienkiewicz and Taylor, 2000).

OUTLINE OF NEW PLATE THEORY

Deformation of a thick rectangular plate is considered in the Cartesian coordinate system in Fig. 1. By following the idea from the modified Timoshenko beam theory, total deflection is decomposed into bending deflection and shear deflection (Senjanović et al., 2013a; 2013b)

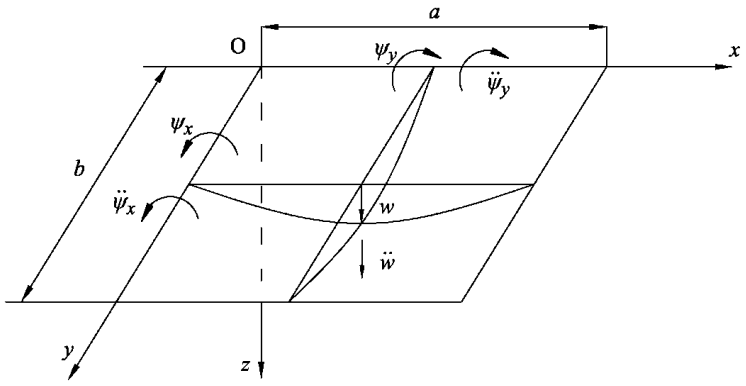

Fig. 1 Displacements of rectangular plate.

$$w(x,y,t)=w_b(x,y,t)+w_s(x,y,t). \tag{1}$$

It is assumed that the angles of rotation of the plate cross-section are caused only by bending that is acceptable for the vibration of moderately thick plates in a lower frequency domain

$$\psi_x=-\frac{\partial w_b}{\partial x},\quad \psi_y=-\frac{\partial w_b}{\partial y}. \tag{2}$$

Bending moments and twist moments are a function of plate curvatures and warping, respectively, i.e.

$$M_x=-D\left(\frac{\partial^2 w_b}{\partial x^2}+\nu\frac{\partial^2 w_b}{\partial y^2}\right), \tag{3}$$

$$M_y=-D\left(\frac{\partial^2 w_b}{\partial y^2}+\nu\frac{\partial^2 w_b}{\partial x^2}\right), \tag{4}$$

$$M_{xy}=M_{yx}=-(1-\nu)D\frac{\partial^2 w_b}{\partial x\partial y}, \tag{5}$$

where

$$D=\frac{Eh^3}{12(1-\nu^2)} \tag{6}$$

is plate flexural rigidity, and h, E and ν is plate thickness, Young's modulus of elasticity and Poisson's ratio, respectively.

Shear strain is the summation of the angle of rotation of the plate generatrix and its cross-section, i.e.

$$\gamma_x=\frac{\partial w}{\partial x}+\psi_x=\frac{\partial w_s}{\partial x}, \tag{7}$$

$$\gamma_y=\frac{\partial w}{\partial y}+\psi_y=\frac{\partial w_s}{\partial y}. \tag{8}$$

Thus, the shear forces read

$$Q_x=S\frac{\partial w_s}{\partial x},\quad Q_y=S\frac{\partial w_s}{\partial y}, \tag{9}$$

where $S=kGh$ is shear rigidity and k is shear coefficient.

Natural vibrations of plate is caused by inertia force and moments

$$q = m\frac{\partial^2 w}{\partial t^2}, \quad m_x = -J\frac{\partial^3 w_b}{\partial x \partial t^2}, \quad m_y = -J\frac{\partial^3 w_b}{\partial y \partial t^2}, \tag{10}$$

where $m = \rho h$ is the plate mass per unit area, and $J = \rho I = \rho h^3/12$ is the mass moment of inertia of the cross-section per unit breadth.

By considering the equilibrium of vertical forces and moments around the *x* and *y* axis, and applying the above relations, one obtains a single differential equation of motion as shown in (Senjanović et al., 2013a)

$$D\Delta\Delta w_b - J\left(1+\frac{mD}{JS}\right)\frac{\partial^2}{\partial t^2}\Delta w_b + m\frac{\partial^2}{\partial t^2}\left(w_b + \frac{J}{mS}\frac{\partial^2 w_b}{\partial t^2}\right) = q(x,y,t), \tag{11}$$

where $\Delta(.) = \frac{\partial^2(.)}{\partial x^2} + \frac{\partial^2(.)}{\partial y^2}$ is the Laplace differential operator and q is the distributed excitation. Bending deflection w_b is actually a potential function since the remaining displacements w_s, ψ_x and ψ_y are defined by its derivatives. Hence, the total deflection (1), according to (Senjanović et al., 2013a) reads

$$w = w_b + \frac{J}{S}\frac{\partial^2 w_b}{\partial t^2} - \frac{D}{S}\Delta w_b. \tag{12}$$

FORMULATION OF FINITE ELEMENT PROPERTIES

A general finite element with *n* nodes and three d.o.f. per node, i.e. deflection and rotations around the *x* and *y* axis, is considered. The ordinary procedure for determining stiffness and the mass matrix in the case of a thin plate is used (Szilard, 2004). Bending deflection as a potential function is assumed in a polynomial form with a number of unknown coefficients which corresponds to the total number of d.o.f. N=3n

$$w_b = \langle a \rangle \{P\}_b, \tag{13}$$

where $\langle a \rangle$ is a row vector with terms a_i, i=0,1,...N-1, and

$$\{P\}_b^T = \langle P \rangle_b = \langle 1, x, y, x^2, xy, y^2 \ldots \rangle. \tag{14}$$

Total static deflection, according to (12), reads

$$w = \langle a \rangle \left(\{P\}_b - \frac{D}{S}\frac{\partial^2 \{P\}_b}{\partial x^2} - \frac{D}{S}\frac{\partial^2 \{P\}_b}{\partial y^2} \right). \tag{15}$$

Angles of rotation (2) yield

$$\psi_x = -\langle a \rangle \frac{\partial \{P\}_b}{\partial x}, \quad \psi_y = -\langle a \rangle \frac{\partial \{P\}_b}{\partial y}. \tag{16}$$

By taking coordinate values x_l and y_l for each node, l=1,2...n , into account in Eqs. (15) and (16), the relation between the nodal displacements and the unknown coefficients a_i is obtained

$$\{\delta\} = [C]\{a\}, \tag{17}$$

where [C] includes x_l and y_l and

$$\{\delta\} = \begin{Bmatrix} \{\delta\}_1 \\ \vdots \\ \{\delta\}_n \end{Bmatrix}, \quad \{\delta\}_l = \begin{Bmatrix} w_l \\ \varphi_l \\ \psi_l \end{Bmatrix}. \tag{18}$$

Now, for the given nodal displacement vector $\{\delta\}$, the corresponding coefficient vector $\{a\}$ can be determined from (17)

$$\{a\} = [C]^{-1}\{\delta\}. \tag{19}$$

Substituting (19) into (13) yields

$$w_b = \langle\phi\rangle_b \{\delta\}, \tag{20}$$

where

$$\langle\phi\rangle_b = \langle P\rangle_b [C]^{-1} \tag{21}$$

is the vector of the bending shape functions.

In a similar way, shear deflection can be presented in the form

$$w_s = \langle P\rangle_s \{a\}, \tag{22}$$

where according to (15)

$$\langle P\rangle_s = -\frac{D}{S}\frac{\partial^2 \langle P\rangle_b}{\partial x^2} - \frac{D}{S}\frac{\partial^2 \langle P\rangle_b}{\partial y^2}. \tag{23}$$

Substituting (19) into (22) yields

$$w_s = \langle\phi\rangle_s \{\delta\}, \tag{24}$$

where

$$\langle\phi\rangle_s = \langle P\rangle_s [C]^{-1} \tag{25}$$

is the vector of the shear shape functions.

Total deflection according to (1) reads

$$w = \langle \phi \rangle \{\delta\}, \tag{26}$$

where

$$\langle \phi \rangle = \langle \phi \rangle_b + \langle \phi \rangle_s \tag{27}$$

is the vector of the total shape functions.

Columns of the inverted matrix [*C*] are vectors of coefficients a_i obtained for the unit value of particular nodal displacements

$$[C]^{-1} = \left[\{A\}_1 \{A\}_2 ... \{A\}_N \right], \tag{28}$$

where

$$\{A\}_j^T = \langle A \rangle_j = \left\langle a_0^j \ a_1^j ... a_{N-1}^j \right\rangle. \tag{29}$$

Bending curvatures and warping are presented in the form

$$\{\kappa\}_b = -\begin{Bmatrix} \dfrac{\partial^2 w_b}{\partial x^2} \\ \dfrac{\partial^2 w_b}{\partial y^2} \\ 2\dfrac{\partial^2 w_b}{\partial x \partial y} \end{Bmatrix}. \tag{30}$$

Substituting (20) with (21) into (30) yields

$$\{\kappa\}_b = -[L]_b \{\delta\}, \tag{31}$$

where

$$[L]_b = [H]_b [C]^{-1}, \tag{32}$$

$$[H]_b = \begin{bmatrix} \dfrac{\partial^2 \langle P \rangle_b}{\partial x^2} \\ \dfrac{\partial^2 \langle P \rangle_b}{\partial y^2} \\ 2\dfrac{\partial^2 \langle P \rangle_b}{\partial x \partial y} \end{bmatrix}. \tag{33}$$

Now it is possible to determine the bending stiffness matrix by employing a general formulation from the finite element method based on the variational principle as shown in (Zienkiewicz and Taylor, 2000)

$$[K]_b = \int_A [L]_b^T [D]_b [L]_b \, dA, \tag{34}$$

where

$$[D]_b = D \begin{bmatrix} 1 & \nu & 0 \\ \nu & 1 & 0 \\ 0 & 0 & \frac{1-\nu}{2} \end{bmatrix} \tag{35}$$

is the matrix of plate flexural rigidity. Furthermore, substituting (32) with (33) into (34) yields

$$[K]_b = [C]^{-T} [B] [C]^{-1}, \tag{36}$$

where symbolically $[C]^{-T} = \left([C]^{-1}\right)^T$ and

$$[B] = \int_A [H]_b^T [D]_b [H]_b \, dA. \tag{37}$$

By taking (33) and (35) into account, (37) can be presented in the form

$$[B] = D\left([I]_1 + \nu\left([I]_2 + [I]_3\right) + [I]_4 + 2(1-\nu)[I]_5\right), \tag{38}$$

where

$$[I]_1 = \int_A \frac{\partial^2 \{P\}_b}{\partial x^2} \frac{\partial^2 \langle P \rangle_b}{\partial x^2} dA, \tag{39}$$

$$[I]_2 = \int_A \frac{\partial^2 \{P\}_b}{\partial x^2} \frac{\partial^2 \langle P \rangle_b}{\partial y^2} dA = [I]_3^T, \tag{40}$$

$$[I]_4 = \int_A \frac{\partial^2 \{P\}_b}{\partial y^2} \frac{\partial^2 \langle P \rangle_b}{\partial y^2} dA, \tag{41}$$

$$[I]_5 = \int_A \frac{\partial^2 \{P\}_b}{\partial x \partial y} \frac{\partial^2 \langle P \rangle_b}{\partial x \partial y} dA. \tag{42}$$

According to (9) the shear strain vector reads

$$\{\gamma\} = \begin{Bmatrix} \dfrac{\partial w_s}{\partial x} \\ \dfrac{\partial w_s}{\partial y} \end{Bmatrix}, \tag{43}$$

and by taking (24) with (25) into account, one obtains

$$\{\gamma\} = [L]_s \{\delta\}, \tag{44}$$

where

$$[L]_s = [H]_s [C]^{-1}, \tag{45}$$

$$[H]_s = \begin{bmatrix} \dfrac{\partial \langle P \rangle_s}{\partial x} \\ \dfrac{\partial \langle P \rangle_s}{\partial y} \end{bmatrix}. \tag{46}$$

Analogously to (34), the shear stiffness matrix is presented in the form

$$[K]_s = \int_A [L]_s^T [D]_s [L]_s \, \mathrm{d}A, \tag{47}$$

where $[D]_s = S \begin{bmatrix} 1 & 0 \\ 0 & 1 \end{bmatrix}$. Substituting (45) with (46) into (47) yields

$$[K]_s = [C]^{-T} [S] [C]^{-1}, \tag{48}$$

where

$$[S] = S \int_A [H]_s^T [H]_s \, \mathrm{d}A. \tag{49}$$

By taking (46) into account, (49) can be presented in the form

$$[S] = S \left([I]_6 + [I]_7 \right), \tag{50}$$

where

$$[I]_6 = \int_A \frac{\partial \{P\}_s}{\partial x} \frac{\partial \langle P \rangle_s}{\partial x} \mathrm{d}A, \tag{51}$$

$$[I]_7 = \int_A \frac{\partial \{P\}_s}{\partial y} \frac{\partial \langle P \rangle_s}{\partial y} \mathrm{d}A. \tag{52}$$

Hence, the complete stiffness matrix is

$$[K] = [K]_b + [K]_s = [C]^{-T} ([B] + [S])[C]^{-1}. \tag{53}$$

According to the general formulation of the mass matrix in the finite element method based on the variational principle (Zienkiewicz and Taylor, 2000), one can write

$$[M] = m \int_A \{\phi\} \langle \phi \rangle \mathrm{d}A, \tag{54}$$

where $\{\phi\}$ is the vector of the total shape functions (27). Taking (21) and (25) into account yields

$$[M] = m[C]^{-T} [I]_0 [C]^{-1}, \tag{55}$$

where

$$[I]_0 = \int_A \{P\} \langle P \rangle \mathrm{d}A, \tag{56}$$

and $\{P\} = \{P\}_b + \{P\}_s$, Eqs. (14) and (23).

RELATIONSHIP BETWEEN THICK AND THIN FINITE ELEMENT PROPERTIES

If the shape functions of thick and thin plate are determined by the same polynomial, it is interesting to find out the relation between their properties. For this purpose, let us decompose the coefficient matrix [*C*] into the bending matrix and shear contribution

$$[C] = [C]_b + [C]_s, \tag{57}$$

where $[C]_b$ includes all terms without shear stiffness *S*, while $[C]_s$ contains only terms with *S*. Eq. (57) can also be presented in the form

$$[C] = ([I] + [E])[C]_b, \tag{58}$$

where [*I*] is the identity matrix and

$$[E]=[C]_s[C]_b^{-1}. \tag{59}$$

Furthermore, substituting (58) into (36) and employing the inverse of the product, $\left([A][B]\right)^{-1}=[B]^{-1}[A]^{-1}$, and the transpose of the product, $\left([A][B]\right)^{T}=[B]^{T}[A]^{T}$, one arrives at

$$[K]_b=\left([I]+[E]^{T}\right)^{-1}[K]_b^0\left([I]+[E]\right)^{-1}, \tag{60}$$

where

$$[K]_b^0=[C]_b^{-T}[B][C]_b^{-1} \tag{61}$$

is the bending stiffness matrix of thin plate.

In a similar way, the matrix of shear stiffness (48) can be presented in the form (60), and the complete stiffness matrix of thick plate reads

$$[K]=\left([I]+[E]^{T}\right)^{-1}\left([K]_b^0+[K]_s^0\right)\left([I]+[E]\right)^{-1}, \tag{62}$$

where

$$[K]_s^0=[C]_b^{-T}[S][C]_b^{-1}. \tag{63}$$

The mass matrix (55) can also be decomposed if the relation $\{P\}=\{P\}_b+\{P\}_s$ is taken into account. Hence, one obtains

$$[M]=\left([I]+[E]^{T}\right)^{-1}\left([M]_b+[M]_{bs}+[M]_{sb}+[M]_s\right)\left([I]+[E]\right)^{-1}, \tag{64}$$

where

$$[M]_b=m[C]_b^{-T}\int_A\{P\}_b\langle P\rangle_b\,\mathrm{d}A[C]_b^{-1}, \tag{65}$$

$$[M]_{bs}=m[C]_b^{-T}\int_A\{P\}_b\langle P\rangle_s\,\mathrm{d}A[C]_b^{-1}=[M]_{sb}^{T}, \tag{66}$$

$$[M]_s=m[C]_b^{-T}\int_A\{P\}_s\langle P\rangle_s\,\mathrm{d}A[C]_b^{-1}. \tag{67}$$

The matrix $[M]_b$ is the bending mass matrix of thin plate, $[M]_s$ is the shear mass matrix of thick plate, and $[M]_{bs}$ and $[M]_{sb}$ are mass matrices of bending and shear coupling.

Distributed excitation is transmitted to the nodes by the shape functions

$$\{F\} = \int_A \{\phi\}\, q\mathrm{d}A\,. \tag{68}$$

Taking (21) and (25) into account yields

$$\{F\} = [C]^{-T} \int_A \{P\}\, q\mathrm{d}A\,. \tag{69}$$

Furthermore, by employing (58) and $\{P\} = \{P\}_b + \{P\}_s$, one arrives at

$$\{F\} = \left([I] + [E]^T\right)^{-1} \left(\{F\}_b + \{F\}_s\right), \tag{70}$$

where

$$\{F\}_b = [C]_b^{-T} \int_A \{P\}_b\, q\mathrm{d}A \tag{71}$$

$$\{F\}_s = [C]_b^{-T} \int_A \{P\}_s\, q\mathrm{d}A \tag{72}$$

are the vector of the nodal forces due to bending and shear, respectively.

An observation on the relevant literature related to the above subject is given in Appendix.

RECTANGULAR FINITE ELEMENT

The four-node rectangular finite element with nodal displacements is shown in Fig. 2. The dimensionless coordinates $\xi = x/a$ and $\eta = y/b$ are introduced. The ordinary polynomial for the thin plate finite element is applied for bending (Holand and Bell, 1970).

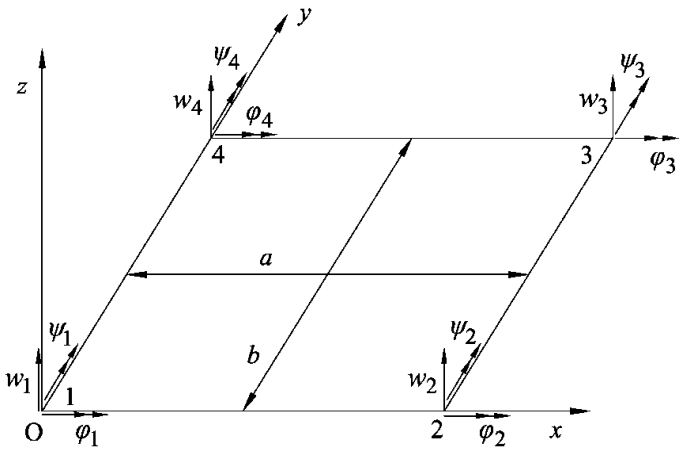

Fig. 2 Rectangular finite element.

$$\langle P\rangle_b = \langle 1,\xi,\eta,\xi^2,\xi\eta,\eta^2,\xi^3,\xi^2\eta,\xi\eta^2,\eta^3,\xi^3\eta,\xi\eta^3\rangle . \tag{73}$$

The shear polynomial according to (23) reads

$$\langle P\rangle_s = -\langle 0,0,0,2\alpha,0,2\beta,6\alpha\xi,2\alpha\eta,2\beta\xi,6\beta\eta,6\alpha\xi\eta,6\beta\xi\eta\rangle , \tag{74}$$

where

$$\alpha = \frac{D}{Sa^2}, \quad \beta = \frac{D}{Sb^2} . \tag{75}$$

$\{P\}_s$ is for two order lower polynomial than $\{P\}_b$ which is important for the possible avoidance of shear locking. The total deflection, Eq. (15), is

$$w = \langle a\rangle\left(\{P\}_b + \{P\}_s\right), \tag{76}$$

and the angles of rotation. Eqs. (16)

$$\psi_x = -\frac{1}{a}\langle a\rangle\frac{\partial\{P\}_b}{\partial\xi}, \quad \psi_y = -\frac{1}{b}\langle a\rangle\frac{\partial\{P\}_b}{\partial\eta} . \tag{77}$$

By taking the coordinates ξ_l and η_l defined in Fig. 2 into account, matrix [*C*] is obtained in the following form

$$[C] = \begin{bmatrix}
1 & 0 & 0 & -2\alpha & 0 & -2\beta & 0 & 0 & 0 & 0 & 0 & 0 \\
0 & 0 & \frac{1}{b} & 0 & 0 & 0 & 0 & 0 & 0 & 0 & 0 & 0 \\
0 & -\frac{1}{a} & 0 & 0 & 0 & 0 & 0 & 0 & 0 & 0 & 0 & 0 \\
1 & 1 & 0 & 1-2\alpha & 0 & -2\beta & 1-6\alpha & 0 & -2\beta & 0 & 0 & 0 \\
0 & 0 & \frac{1}{b} & 0 & \frac{1}{b} & 0 & 0 & \frac{1}{b} & 0 & 0 & \frac{1}{b} & 0 \\
0 & -\frac{1}{a} & 0 & -\frac{2}{a} & 0 & 0 & -\frac{3}{a} & 0 & 0 & 0 & 0 & 0 \\
1 & 1 & 1 & 1-2\alpha & 1 & 1-2\beta & 1-6\alpha & 1-2\alpha & 1-2\beta & 1-6\beta & 1-6\alpha & 1-6\beta \\
0 & 0 & \frac{1}{b} & 0 & \frac{1}{b} & \frac{2}{b} & 0 & \frac{1}{b} & \frac{2}{b} & \frac{3}{b} & \frac{1}{b} & \frac{3}{b} \\
0 & -\frac{1}{a} & 0 & -\frac{2}{a} & -\frac{1}{a} & 0 & -\frac{3}{a} & -\frac{2}{a} & -\frac{1}{a} & 0 & -\frac{3}{a} & -\frac{1}{a} \\
1 & 0 & 1 & -2\alpha & 0 & 1-2\beta & 0 & -2\alpha & 0 & 1-6\beta & 0 & 0 \\
0 & 0 & \frac{1}{b} & 0 & 0 & \frac{2}{b} & 0 & 0 & 0 & \frac{3}{b} & 0 & 0 \\
0 & -\frac{1}{a} & 0 & 0 & -\frac{1}{a} & 0 & 0 & 0 & -\frac{1}{a} & 0 & 0 & -\frac{1}{a}
\end{bmatrix} . \tag{78}$$

The stiffness and mass matrix can be determined directly by employing Eqs. (53) and (55), respectively, or in an indirect way by Eqs. (62) and (64). The decomposition of matrix [C] into $[C]_b$ and $[C]_s$ is very simple. The inversion of the matrices can be done analytically by a Computer Algebra System (CAS). For illustration, matrix [E] is obtained in the following form:

$$[E]=\begin{bmatrix} 6\alpha+6\beta & 4b\beta & -4a\alpha & -6\alpha & 0 & -2a\alpha & 0 & 0 & 0 & -6\beta & 2b\beta & 0 \\ 0 & 0 & 0 & 0 & 0 & 0 & 0 & 0 & 0 & 0 & 0 & 0 \\ 0 & 0 & 0 & 0 & 0 & 0 & 0 & 0 & 0 & 0 & 0 & 0 \\ -6\alpha & 0 & 2a\alpha & 6\alpha+6\beta & 4b\beta & 4a\alpha & -6\beta & 2b\beta & 0 & 0 & 0 & 0 \\ 0 & 0 & 0 & 0 & 0 & 0 & 0 & 0 & 0 & 0 & 0 & 0 \\ 0 & 0 & 0 & 0 & 0 & 0 & 0 & 0 & 0 & 0 & 0 & 0 \\ 0 & 0 & 0 & -6\beta & -2b\beta & 0 & 6\alpha+6\beta & -4b\beta & 4a\alpha & -6\alpha & 0 & 2a\alpha \\ 0 & 0 & 0 & 0 & 0 & 0 & 0 & 0 & 0 & 0 & 0 & 0 \\ 0 & 0 & 0 & 0 & 0 & 0 & 0 & 0 & 0 & 0 & 0 & 0 \\ -6\beta & -2b\beta & 0 & 0 & 0 & 0 & -6\alpha & 0 & -2a\alpha & 6\alpha+6\beta & -4b\beta & -4a\alpha \\ 0 & 0 & 0 & 0 & 0 & 0 & 0 & 0 & 0 & 0 & 0 & 0 \\ 0 & 0 & 0 & 0 & 0 & 0 & 0 & 0 & 0 & 0 & 0 & 0 \end{bmatrix}. \quad (79)$$

TRIANGULAR FINITE ELEMENT

The three-node triangular finite element in the Cartesian coordinate system with nodal displacements is shown in Fig. 3. The ordinary polynomial for triangular finite element of thin plate is used for bending

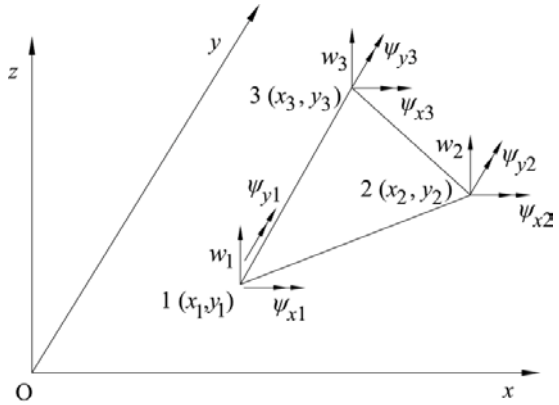

Fig. 3 Triangular finite element.

$$\langle P\rangle_b=\langle 1,x,y,x^2,xy,y^2,x^3,x^2y+xy^2,y^3\rangle, \quad (80)$$

The shear polynomial is obtained according to (23)

$$\langle P\rangle_s=-\frac{D}{S}\langle 0,0,0,2,0,2,6x,2(x+y),6y\rangle. \quad (81)$$

The total deflection is

$$w=\langle a\rangle\left(\{P\}_b+\{P\}_s\right), \quad (82)$$

where $\langle a\rangle = \langle 0, a_1, ..., a_8\rangle$. Angles of rotation are determined according to (16), i.e.

$$\begin{aligned}\psi_x &= -\langle a\rangle\{0,1,0,2x,y,0,3x^2,2xy+y^2,0\}\\ \psi_y &= -\langle a\rangle\{0,0,1,0,x,2y,0,x^2+2xy,3y^2\}.\end{aligned} \tag{83}$$

Matrix [*C*] in expression for nodal displacements, Eqs. (17) and (18), is obtained by taking nodal coordinates x_l and y_l, l=1,2,3, into account

$$[C]=\begin{bmatrix}
1 & x_1 & y_1 & x_1^2-2\frac{D}{S} & x_1y_1 & y_1^2-2\frac{D}{S} & x_1^3-6\frac{D}{S}x_1 & x_1^2y_1+x_1y_1^2-2\frac{D}{S}(x_1+y_1) & y_1^3-6\frac{D}{S}y_1\\
0 & -1 & 0 & -2x_1 & -y_1 & 0 & -3x_1^2 & -(2x_1y_1+y_1^2) & 0\\
0 & 0 & -1 & 0 & -x_1 & -2y_1 & 0 & -(x_1^2+2x_1y_1) & -3y_1^2\\
1 & x_2 & y_2 & x_2^2-2\frac{D}{S} & x_2y_2 & y_2^2-2\frac{D}{S} & x_2^3-6\frac{D}{S}x_2 & x_2^2y_2+x_2y_2^2-2\frac{D}{S}(x_2+y_2) & y_2^3-6\frac{D}{S}y_2\\
0 & -1 & 0 & -2x_2 & -y_2 & 0 & -3x_2^2 & -(2x_2y_2+y_2^2) & 0\\
0 & 0 & -1 & 0 & -x_2 & -2y_2 & 0 & -(x_2^2+2x_2y_2) & -3y_2^2\\
1 & x_3 & y_3 & x_3^2-2\frac{D}{S} & x_3y_3 & y_3^2-2\frac{D}{S} & x_3^3-6\frac{D}{S}x_3 & x_3^2y_3+x_3y_3^2-2\frac{D}{S}(x_3+y_3) & y_3^3-6\frac{D}{S}y_3\\
0 & -1 & 0 & -2x_3 & -y_3 & 0 & -3x_3^2 & -(2x_3y_3+y_3^2) & 0\\
0 & 0 & -1 & 0 & -x_3 & -2y_3 & 0 & -(x_3^2+2x_3y_3) & -3y_3^2
\end{bmatrix}. \tag{84}$$

In order to determine bending stiffness matrix it is necessary to define matrix $[H]_b$, Eq. (33). Hence, one finds

$$[H]_b=\begin{bmatrix}0&0&0&2&0&0&6x&2y&0\\0&0&0&0&0&1&0&2x&6y\\0&0&0&0&2&0&0&4(x+y)&0\end{bmatrix}. \tag{85}$$

Matrix [*B*], Eq. (37), in the bending stiffness matrix, Eq. (36), is given in the Cartesian coordinate system. In order to make integration over the element area possible, triangular coordinates ξ and η are introduced. According to Fig. 4 one can write

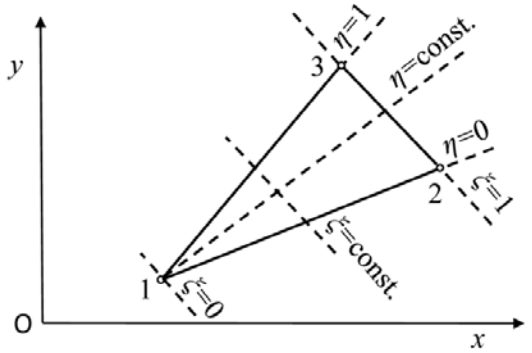

Fig. 4 Triangular coordinates.

$$x = x_1 + x_{21}\xi + x_{32}\xi\eta$$
$$y = y_1 + y_{21}\xi + y_{32}\xi\eta, \tag{86}$$

where $x_{ij} = x_i - x_j$ and $y_{ij} = y_i - y_j$. Furthermore, differential area of triangular element reads

$$\mathrm{d}A = J\mathrm{d}\xi\mathrm{d}\eta, \tag{87}$$

where

$$J = \begin{vmatrix} \dfrac{\partial x}{\partial \xi} & \dfrac{\partial x}{\partial \eta} \\ \dfrac{\partial y}{\partial \xi} & \dfrac{\partial y}{\partial \eta} \end{vmatrix} = 2A\xi \tag{88}$$

is Jacobian and $A = \dfrac{1}{2}\left(x_{21}y_{31} - x_{31}y_{21}\right)$ is element area. Finally, one can write for matrix [B], Eq. (37)

$$[B] = 2A\int_0^1\int_0^1 \left[H(\xi,\eta)\right]_b^T [D]_b \left[H(\xi,\eta)\right]_b \mathrm{d}\xi\mathrm{d}\eta. \tag{89}$$

In a similar way matrix $[H]_s$, Eq. (46), in the shear stiffness matrix, Eqs. (48) and (49), takes the following constant form

$$[H]_s = -\frac{D}{S}\begin{bmatrix} 0 & 0 & 0 & 0 & 0 & 0 & 6 & 2 & 0 \\ 0 & 0 & 0 & 0 & 0 & 0 & 0 & 2 & 6 \end{bmatrix} \tag{90}$$

Hence, one finds for matrix [*S*], Eq. (49), after integration

$$[S] = AS[H]_s^T [H]_s = \left(\frac{D}{S}\right)^2 \begin{bmatrix} [0] & [0] \\ [0] & [s] \end{bmatrix}, \tag{91}$$

where

$$[s] = \begin{bmatrix} 36 & 12 & 0 \\ 12 & 8 & 12 \\ 0 & 12 & 36 \end{bmatrix}. \tag{92}$$

Mass matrix [*M*] is defined by Eqs. (55) and (56), where by employing triangular coordinates

$$[I]_0 = 2A\int_0^1\int_0^1 \left\{P(\xi,\eta)\right\}\left\langle P(\xi,\eta)\right\rangle \xi\mathrm{d}\xi\mathrm{d}\eta. \tag{93}$$

and $\left\{P(\xi,\eta)\right\} = \left\{P(\xi,\eta)\right\}_b + \left\{P(\xi,\eta)\right\}_s$.

It is necessary to mention that application of the triangular coordinates in case that two element boundaries are parallel to the coordinate axes leads to singularity of element properties. Therefore, application of the area coordinates is preferable in general case (Zienkiewicz, 1971).

NUMERICAL EXAMPLES

Reliability of the developed finite element formulation and four noded rectangular element is analysed by three numerical examples of natural vibrations: simply supported square plate (SSSS), rectangular plate clamped on transverse edges and simply supported on longitudinal edges (CSCS), and rectangular plate for combined clamped, free, and simply supported boundary conditions (CFSS). All plates are modelled with 8×8=64 finite elements. Necessary data and nondimensional frequency parameters are listed in the title of Tables 1, 2 and 3. Thin and thick plates are considered and Present Solutions (PS) are compared with available ones determined analytically, Tables 1 and 2, and by Rayleigh-Ritz method, Table 3. Also, results obtained by NASTRAN (MSC, 2010) are included in the tables. In the most cases very high accuracy is achieved, somewhere better than that of NASTRAN results. PS and NASTRAN values for thick plates bound rigorous frequency parameters. The first four natural nodes for case CFSS generated by NASTRAN are shown in Fig. 5 for illustration.

Table 1 Frequency parameter $\mu = \omega a^2 \sqrt{\rho h / D}$ of square plate, case SSSS, k=0.86667.

h/a	Method	1/11/*	2/12/	3/21/	4/22/	5/13/	6/31/	7/23/	8/32/
0.001	Hashemi and Arsanjani (2005)	19.739	49.348	49.348	78.956	98.694	98.693	128.302	128.302
	Senjanović et al. (2013a)	19.739	49.348	49.348	78.956	98.694	98.694	128.302	128.302
	FEM – PS	19.592	48.744	48.744	76.603	98.487	98.487	123.374	123.374
	FEM – NASTRAN	19.377	48.115	48.115	74.420	96.381	96.381	119.255	119.255
0.1	Hashemi and Arsanjani* (2005)	19.084	45.585	45.585	70.022	85.365	85.365	107.178	107.178
	Senjanović et al. (2013a)	19.084	45.585	45.585	70.022	85.365	85.365	107.177	107.177
	FEM – PS	19.082	45.924	45.924	70.134	87.655	87.655	108.510	108.510
	FEM – NASTRAN	18.274	44.047	44.047	64.502	83.076	83.132	97.0710	97.071
0.2	Hashemi and Arsanjani (2005)	17.506	38.385	38.385	55.586	65.719	65.719	79.476	79.476
	Senjanović et al. (2013a)	17.506	38.385	38.385	55.586	65.719	65.719	79.476	79.476
	FEM - PS	17.795	39.718	39.718	57.512	69.795	69.795	83.561	83.561
	FEM - NASTRAN	16.604	37.414	37.414	51.803	63.932	64.062	72.406	72.406

*/*m*,*n*/ - mode identification number, *m* and *n* number of half waves in *x* and *y* direction.

Table 2 Frequency parameter $\lambda = \left(\omega b^2 / \pi^2\right) \sqrt{\rho h / D}$ of rectangular plate, case CSCS, $a / b = 0.5$, k=0.86667.

h/b	Method	1	2	3	4	5	6	7	8
0.01	Xing & Liu (2009)	9.622	11.691	15.777	22.076	25.573	27.891	30.545	31.969
	Senjanović et al. (2013a)	9.622	11.691	15.777	22.076	25.573	27.891	30.545	31.969
	FEM - PS	9.507	11.287	15.060	21.146	25.292	26.739	29.593	29.648
	FEM - NASTRAN	9.455	11.053	14.538	20.373	25.168	26.323	28.582	28.689
0.1	Xing & Liu (2009)	7.589	9.034	11.948	16.193	16.854	18.117	20.389	21.199
	Senjanović et al. (2013a)	7.589	9.034	11.948	16.139	16.854	18.117	20.389	21.199
	FEM - PS	7.626	9.014	12.044	16.734	17.341	18.390	20.540	22.883
	FEM - NASTRAN	7.541	8.723	11.269	14.920	16.765	17.313	18.418	18.929
0.2	Xing & Liu (2009)	5.202	6.223	8.261	10.350	10.898	11.209	12.706	13.809
	Senjanović et al. (2013a)	5.202	6.223	8.261	10.350	10.898	11.209	12.706	13.809
	FEM - PS	5.327	6.457	8.711	10.936	11.807	11.836	13.378	15.618
	FEM - NASTRAN	5.250	6.202	7.970	10.056	10.402	10.851	11.614	11.994

Table 3 Frequency parameter $\lambda = \left(\omega b^2 / \pi^2\right)\sqrt{\rho h / D}$ of rectangular plate, case CFSS, $a / b = 0.4$, k=5/6.

h/b	Method	1	2	3	4	5	6	7	8
0.001	Liew et al. (1993)	9.874	11.346	14.900	19.539	26.624	31.698	33.397	35.788
	FEM - PS	9.896	11.172	14.017	18.746	25.554	31.711	32.663	34.556
	FEM - NASTRAN	9.823	10.945	13.363	17.404	23.574	31.402	32.257	32.623
0.1	Liew et al. (1993)	7.941	8.970	11.135	14.462	18.761	20.459	21.357	23.112
	FEM - PS	8.099	8.965	11.001	14.476	19.419	21.383	21.931	23.242
	FEM - NASTRAN	7.985	8.635	10.196	12.825	16.215	19.771	20.457	20.887
0.2	Liew et al. (1993)	5.594	6.305	7.752	9.828	12.294	12.679	13.236	14.289
	FEM - PS	5.765	6.386	7.885	10.325	13.418	13.541	13.830	14.757
	FEM - NASTRAN	5.669	6.126	7.277	8.993	10.839	12.470	12.790	12.945

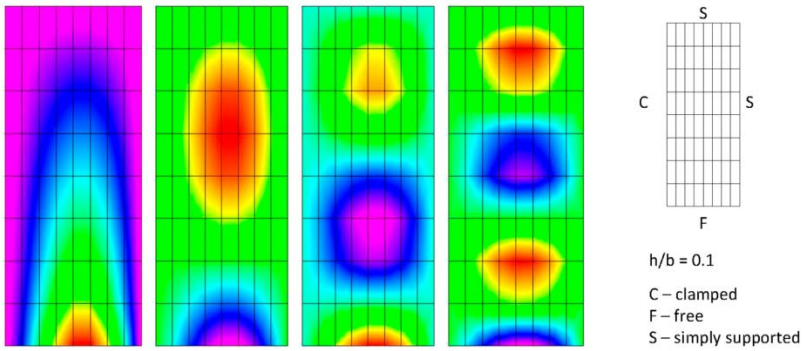

Fig. 5 The first four natural modes of rectangular plate, case CFSS (NASTRAN).

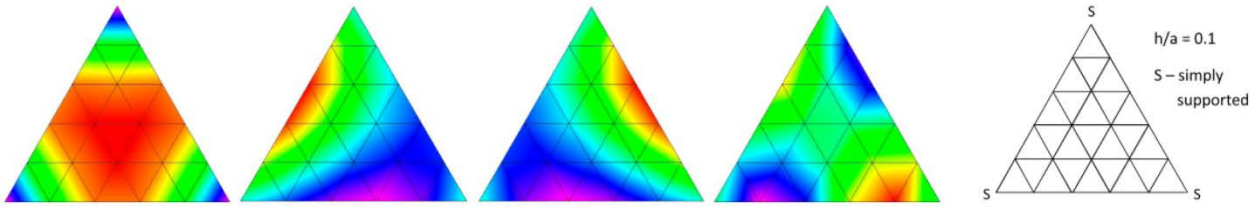

Fig. 6 The first four natural modes of triangular plate with simply supported corner nodes, (NASTRAN).

In addition, the natural vibration of equilateral triangular plate (like tension leg platform), using the developed general triangular finite element is analysed. The plate is modelled with 25 finite elements and it is simply supported at corner nodes. Dimensionless frequency parameters obtained by the proposed procedure are given in Table 4, together with NASTRAN solutions, where good agreement can be noticed. For illustration, the first four natural modes obtained by NASTRAN are shown in Fig. 6.

The convergence of the proposed finite element formulation is demonstrated in the case of a simply supported square plate. Natural frequencies are determined by the finite element model for three mesh densities, i.e. 6×6=36, 8×8=64 and 10x10=100 elements, and three values of a thickness ratio h/a: 0.001, 0.1 and 0.2. The obtained frequency parameters are listed in Table 5 and compared with the exact analytical solution as well as with the NASTRAN and Abaqus (Dassault Systémes, 2008) results. In order to have better insight into the convergence, frequency parameter for the 1st, 4th and 7th modes are shown in Fig. 7. For thin plate (h/a=0.001), the present solution converges to the exact value, faster than the NASTRAN and Abaqus results, which converge from the opposite sides. PS values for moderately thick plate (h/a=0.1) are very close to the exact values for all three mesh densities, while the NASTRAN and Abacus results converge to a lower value than the exact solution. The discrepancy is reduced for higher modes. In the case of thick plate (h/a=0.2), the variation of the PS values, which are somewhat higher than the exact solution, is rather small. The NASTRAN and Abaqus results show the same tendency as in the previous case.

Table 4 Frequency parameter $\mu = \omega a^2 \sqrt{\rho h / D}$ of equilateral triangular plate with simply supported corner nodes, *k*=5/6.

h/a	Method	1	2	3	4	5	6
0.01	FEM - PS	8.691	18.840	18.848	47.014	47.112	64.268
	FEM - NASTRAN	8.542	18.226	18.227	46.990	46.993	63.360
0.1	FEM - PS	8.340	17.821	17.824	43.999	44.002	46.014
	FEM - NASTRAN	8.284	17.609	17.610	43.620	43.624	45.626

Table 5 Convergence of frequency parameter $\mu = \omega a^2 \sqrt{\rho h / D}$ of square plate, case SSSS, *k*=5/6.

h/a	METHOD	1/11/*	2/12/	3/21/	4/22/	5/13/	6/31/	7/23/	8/32/
0.001	Senjanović et al. (2013a)	19.739	49.348	49.348	78.956	98.694	98.694	128.302	128.302
	PS (6×6)	19.459	48.326	48.326	75.103	96.867	96.867	120.658	120.658
	PS (8×8)	19.592	48.744	48.744	76.603	98.487	98.487	123.374	123.374
	PS (10×10)	19.629	48.944	48.944	77.384	97.859	97.859	124.933	124.933
	NASTRAN (6×6)	19.150	47.343	47.343	71.762	95.014	95.084	115.491	115.491
	NASTRAN (8×8)	19.377	48.115	48.115	74.420	96.381	96.381	119.255	119.255
	NASTRAN (10×10)	19.488	48.497	48.497	75.803	97.063	97.063	122.044	122.044
	Abaqus (6×6)	20.205	54.743	54.743	86.623	132.223	132.223	158.355	158.355
	Abaqus (8×8)	20.000	52.251	52.251	83.203	115.389	115.389	143.839	143.839
	Abaqus (10×10)	19.906	51.169	51.169	81.652	124.895	124.895	137.892	137.892
0.1	Senjanović et al. (2013a)	19.065	45.483	45.483	69.794	85.038	85.038	106.684	106.684
	PS (6×6)	18.959	45.581	45.581	69.055	87.636	87.636	107.334	107.334
	PS (8×8)	19.063	45.821	45.821	69.908	87.320	87.320	108.019	108.019
	PS (10×10)	19.117	45.949	45.949	70.374	87.230	87.230	108.520	108.520
	NASTRAN (6×6)	18.022	42.985	42.985	60.972	80.069	80.090	89.787	89.787
	NASTRAN (8×8)	18.243	43.927	43.927	64.251	82.692	82.750	96.541	96.541
	NASTRAN (10×10)	18.339	44.380	44.380	65.918	83.926	84.008	100.115	100.115
	Abaqus (6×6)	18.906	49.078	49.078	73.469	106.435	106.605	122.766	122.766
	Abaqus (8×8)	18.663	46.971	46.971	70.836	95.661	95.831	114.072	114.072
	Abaqus (10×10)	18.544	46.037	46.037	69.609	91.190	91.354	110.279	110.279
0.2	Senjanović et al. (2013a)	17.449	38.152	38.152	55.150	65.145	65.145	78.697	78.697
	PS (6×6)	17.662	39.476	39.476	56.997	70.314	70.314	83.630	83.630
	PS (8×8)	17.733	39.454	39.454	57.016	69.123	69.123	82.667	82.667
	PS (10×10)	17.767	39.451	39.451	57.081	68.584	68.584	82.280	82.280
	NASTRAN (6×6)	16.348	36.264	36.264	48.588	60.567	60.641	65.908	65.908
	NASTRAN (8×8)	16.535	37.148	37.148	51.336	63.253	63.383	71.578	71.578
	NASTRAN (10×10)	16.617	37.562	37.562	52.679	64.503	64.667	74.427	74.427
	Abaqus (6×6)	16.796	40.014	40.014	56.260	76.247	76.591	85.787	85.787
	Abaqus (8×8)	16.610	38.620	38.620	54.749	70.632	70.966	81.596	81.596
	Abaqus (10×10)	16.523	37.997	37.997	54.046	68.169	68.493	79.675	79.675

*/*m*,*n*/ - mode identification number, *m* and *n* number of half waves in *x* and *y* direction.

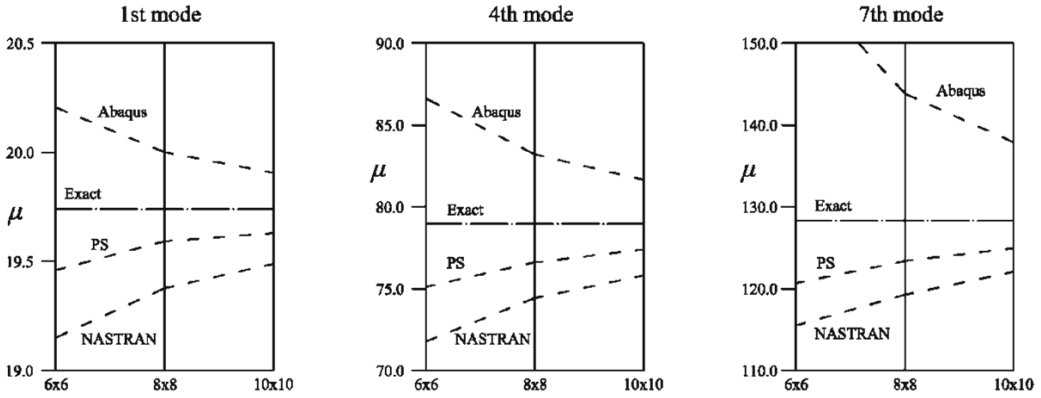

(a) h/a=0.001.

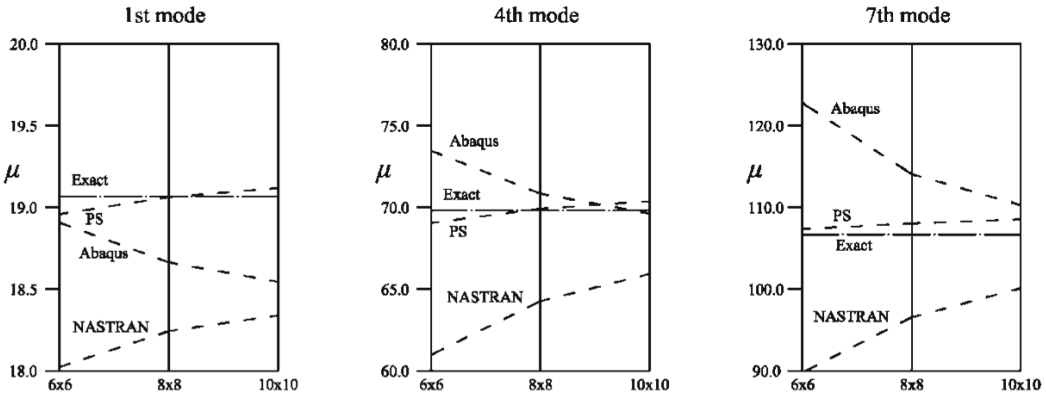

(b) h/a=0.1.

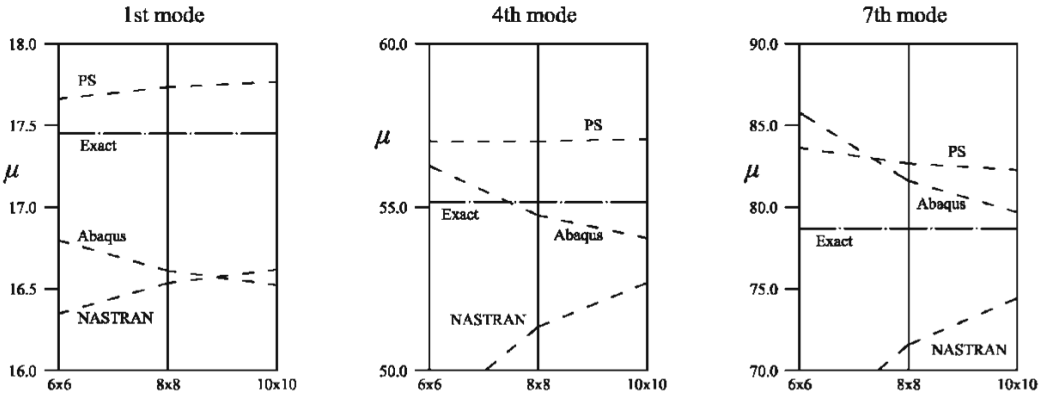

(c) h/a=0.2.

Fig. 7 Convergence of frequency parameter $\mu = \omega a^2 \sqrt{\rho h / D}$ of simply supported square plate, k=5/6.

CONCLUSION

Thick plate appears as a structural element in many engineering structures. In this paper, an outline of the modified Mindlin theory for moderately thick plate is presented. Instead of three variables, i.e. deflection and two rotations of cross-sections, the problem is reduced to only one, where bending deflection is used as a potential function for determining the remaining displacements, strains and sectional forces. A new formulation of thick plate finite elements based on this theory is proposed following the standard FEM procedure, thus ensuring variational consistency. The well-known shear locking problem, which accompanies the Mindlin theory, is overcome as a result of the strong interdependence among deflection and rotations which

reduce the order of the shear polynomial compared to the bending polynomial. The consistent relationship between thick and thin finite element properties is derived, so that the stiffness and mass matrix for the thick element can be determined directly or indirectly. Based on a systematic analysis of this subject, some shortcomings of a known similar relationship are noticed and discussed. The vibration analysis of a thick rectangular plate by a simple quadrilateral finite element and coarse mesh shows a higher level of accuracy than sophisticated finite elements incorporated in some commercial software packages. Developed triangular finite element applied for vibration analysis of the triangular plate, also gives good results. Avoidance of the shear locking problem, fast convergence and high accuracy are the advantages of the proposed finite element formulation for vibration analysis of moderately thick plates.

Shear locking is not a natural phenomenon. It is introduced by the inconsistent mathematical modelling of a physical task, resulting in a numerical problem. With finite elements based on the original Mindlin thick plate theory, it is not possible to ensure smooth transition from thick to thin plate, since the shear stiffness, which is dominant for higher modes, also remains dominant for lower modes, which is not realistic. Any attempt to eliminate shear locking results in complicated finite element properties and a decrease in accuracy. However, such elements can usually capture so-called missing modes in the higher frequency domain, which represent the coupling of ordinary bending-shear modes with in-plane shear modes (Lim et al., 2005). In contrast, the modified Mindlin theory is related to moderately thick plate and due to the strong interdependence among the deflection and rotations the shear locking problem in finite elements does not occur. Finite elements derived according to these two theories actually cover two regions of the problem, i.e. one from thin to moderately thick plates, and the other from moderately to fully thick plates, which partly overlap. Higher accuracy is obtained in the former types of finite elements than in the latter if moderately thick plate is an issue. Based on the above, it is not efficient to derive unique finite elements for solving shear locking and capturing high in-plane modes which are usually not of practical interest. Now, the proposed procedure for the formulation of shear locking-free finite elements may be used for the development of sophisticated thick plate elements with different shapes and a higher number of nodes.

ACKNOWLEDGMENT

This work was supported by a National Research Foundation of Korea (NRF) grant funded by the Korean Government (MSIP) through GCRC-SOP (Grant No. 2011-0030013). The authors express their gratitude to Marko Jokić, DSc, University of Zagreb, for numerical calculations by Abaqus.

REFERENCES

Auricchio, F. and Taylor, R.L., 1995. A triangular thick plate finite element with an exact thin limit. *Finite Elements in Analysis and Design*, 19, pp.57-68.

Bathe, K.J., 1996. *Finite element procedures*. Englewood Cliffs: Prentice-Hall/MIT.

Bletzinger, K., Bischoff, M. and Ramm E., 2000. A unified approach for shear-locking-free triangular and rectangular shell finite elements. *Computers and Structures*, 75(3), pp.321-334.

Cheung, Y.K. and Zhou, D., 2000. Vibrations of moderately thick rectangular plates in terms of a set of static Timoshenko beam functions. *Computers and Structures*, 78(6), pp.757-768.

Cho, D.S., Vladimir, N. and Choi, T.M., 2013. Approximate natural vibration analysis of rectangular plates with openings using assumed mode method. *International Journal of Naval Architecture and Ocean Engineering*, 5(3), pp.478-491.

Cho, D.S., Vladimir, N. and Choi, T.M., 2014. Natural vibration analysis of stiffened panels with arbitrary edge constraints using the assumed mode method. *Proceedings of the IMechE, Part M: Journal of Engineering for the Maritime Environment*. DOI:10.1177/1475090214521179 (published online).

Dassault Systémes, 2008. *Abaqus analysis user's manual. Version 6.8*. Providence, RI, USA: Dassault Systémes.

Dawe, D.J. and Roufaeil, O.L., 1980. Rayleigh-Ritz vibration analysis of Mindlin plates. *Journal of Sound and Vibration*, 69(3), pp.345-359.

Eftekhari, S.A. and Jafari A.A., 2013. A simple and accurate mixed FE-DQ formulation for free vibration of rectangular and skew Mindlin plates with general boundary conditions. *Meccanica*, 48, pp.1139-1160.

Endo, M. and Kimura, N., 2007. An alternative formulation of the boundary value problem for the Timoshenko beam and Mindlin plate. *Journal of Sound and Vibration*, 301(1-2), pp.355-373.

Falsone, G. and Settineri, D., 2011. An Euler-Bernoulli-like finite element method for Timoshenko beams. *Mechanics Research Communications*, 38(1), pp.12-16.

Falsone, G. and Settineri, D., 2012. A Kirchoff-like solution for the Mindlin plate model: A new finite element approach. *Mechanics Research Communications*, 40, pp.1-10.

Hashemi, S.H. and Arsanjani, M., 2005. Exact characteristic equations for some of classical boundary conditions of vibrating moderately thick rectangular plate. *International Journal of Solids and Structures*, 42(3-4), pp.819-853.

Holand, I. and Bell, K., 1970. *Finite element method in stress analysis*. Trondheim: Tapir Forlag.

Hughes, T.J.R., Taylor, R.L. and Kanoknukulchai, W., 1977. Simple and efficient element for plate bending. *International Journal for Numerical Methods in Engineering*, 11(10), pp.1529-1543.

Hughes, T.J.R. and Tezduyar, T., 1981. Finite elements based upon Mindlin plate theory with particular reference to the four-node isoparametric element. *Journal of Applied Mechanics*, 48, pp.587-596.

Kim, K., Kim, B.H., Choi, T.M. and Cho, D.S., 2012. Free vibration analysis of rectangular plate with arbitrary edge constraints using characteristic orthogonal polynomials in assumed mode method. *International Journal of Naval Architecture and Ocean Engineering*, 4(3), pp.267-280.

Lee, S.W. and Wong, X., 1982. Mixed formulation finite elements for Mindlin theory plate bending. *International Journal for Numerical Methods in Engineering*, 18, pp.1297-1311.

Liew, K.M., Xiang, Y. and Kitipornchai, S., 1993. Transverse vibration of thick plates - I. Comprehensive sets of boundary conditions. *Computers and Structures*, 49, pp.1-29.

Liew, K.M., Xiang, Y. and Kitipornchai, S., 1995. Research on thick plate vibration: a literature survey. *Journal of Sound and Vibration*, 180, pp.163-176.

Lim, C.W., Li, Z.R., Xiang, Y., Wei, G.W. and Wang, C.M. 2005. On the missing modes when using the exact frequency relationship between Kirchhoff and Mindlin plates. *Advances in Vibration Engineering*, 4(3), pp.221-248.

Liu, G.R., Nguyen-Thoi, T. and Lam, Y.K., 2009. An edge-based smoothed finite element method (ES-FEM) for static, free and forced vibration analyses of solids. *Journal of Sound and Vibration*, 320(4-5), pp.1100-1130.

Lovadina, C., 1998. Analysis of a mixed finite element method for the Reissner-Mindlin plate problems. *Computer Methods in Applied Mechanics and Engineering*, 163, pp.71-85.

Mindlin, R.D., 1951. Influence of rotary inertia and shear on flexural motions of isotropic elastic plates. *Journal of Applied Mechanics*, 18(1), pp.31-38.

MSC, 2010. *MD Nastran 2010 Dynamic analysis user's guide*. Newport Beach, California, USA: MSC Software.

Nguyen-Xuan, H., Liu, G.R., Thai-Hoang, C. and Nguyen-Thoi, T., 2010. An edge-based smoothed finite element method (ES-FEM) with stabilized discrete shear gap technique for analysis of Reissner-Mindlin plates. *Computer Methods in Applied Mechanics and Engineering*, 199(9-12), pp.471-489.

Reissner, E., 1945. The effect of transverse shear deformation on the bending of elastic plate. *Transactions of ASME Journal of Applied Mechanics*, 12, pp.A69-A77.

Senjanović, I. and Fan, Y., 1989. Investigation of effective bending and shear stiffness of thin-walled girders related to ship hull vibration analysis. *Journal of Ship Research*, 33(4), pp.298-309.

Senjanović, I. and Grubišić, R., 1991. Coupled horizontal and torsional vibrations of a ship hull with large hatch openings. *Computers and Structures*, 41(2), pp.213-226.

Senjanović, I., Tomašević, S. and Vladimir, N., 2009. An advanced theory of thin-walled girders with application to ship vibrations. *Marine Structures*, 22(3), pp.387-437.

Senjanović, I., Vladimir, N. and Tomić, M., 2013a. An advanced theory of moderately thick plate vibrations. *Journal of Sound and Vibration*, 332(7), pp.1868-1880.

Senjanović, I., Tomić, M., Vladimir, N. and Cho, D.S., 2013b. Analytical solution for free vibrations of a moderately thick rectangular plate. *Mathematical Problems in Engineering*, 2013, pp.13.

Senjanović, I. and Vladimir, N., 2013. Physical insight into timoshenko beam theory and its modification with extension. *Structural Engineering and Mechanics*, 48(4), pp.519-545.

Shimpi, R.P. and Patel, H.G., 2006. Free vibrations of plate using two variable refined plate theory, *Journal of Sound and Vibration*, 296, pp.979-999.

Szilard, R., 2004. *Theories and applications of plate analysis*. Hoboken, New Jersey, USA: John Wiley & Sons.

Wang, C.M., 1994. Natural frequencies formula for simply supported Mindlin plates. *ASME Journal of Vibration and Acoustics*, 116, pp.536-540.

Xing, Y. and Liu, B., 2009. Characteristic equations and closed-form solution for free vibrations of rectangular Mindlin plates. *Acta Mechanica Solida Sinica*, 22(2), pp.125-136.

Zienkiewicz, O.C., Taylor, R.L. and To, J.M., 1971. Reduced integration technique in general analysis of plates and shells. *International Journal for Numerical Methods in Engineering*, 3, pp.275-290.

Zienkiewicz, O.C., 1971. *The finite element method in engineering science*. London: McGraw-Hill.

Zienkiewicz, O.C. and Taylor, R.L., 2000. *The finite element method*. 5th ed. Oxford: Butterworth-Heinemann.

APPENDIX – Consideration of the known relationship between thick and thin plate finite element properties

Stiffness matrix of thick plate finite element is derived in (Falsone and Settineri, 2012) by employing the simplified thick plate theory similar to that presented in (Senjanović et al., 2013a). So-called fictitious deflection as single variable is used, which corresponds to the bending deflection applied in the present paper. Stiffness matrix of thick plate finite element is obtained based on the known stiffness matrix of thin plate element. The following relation between those two matrices, written in the present notation, is found:

$$[K]=[K]_b^0\left([I]+[E]\right)^{-1}. \tag{A1}$$

By comparing Eq. (A1) with (62) it is obvious that transformation matrix $\left([I]+[E]^T\right)^{-1}$ on the left side of (62) is not present in (A1). Reason is that shear influence on external nodal forces (70) is ignored in (Falsone and Settineri, 2012), and condition of equivalence of internal nodal forces for thick and thin finite element is used instead of balance of their strain energies. As a result stiffness matrix (A1) is not consistent and consequently it is not symmetric. Relation between equilibrium equations of thick and thin finite element should be of similar form like transformation of element equation from local to global coordinate system (Zienkiewicz and Taylor, 2000). Furthermore, explicitly specified matrix $[S]_b^0$ in (62) is missing in (A1), and the obtained stiffness matrix is not complete. Since this matrix is relevant for shear locking, it is not possible to consider that problem a priori.

Finite element approach to thick plate theory presented in (Falsone and Settineri, 2012) is actually an extension of the previously worked out simplification of the Timoshenko beam theory. Hence, the shortcomings of relation between thick and thin plate finite element properties are also related to the beam elements (Falsone and Settineri, 2011).